J Mater Sci (2011) 46:3378–3386
DOI 10.1007/s10853-010-5226-5

Process optimization and alignment of PVA/$FeCl_3$ nano composite fibres by electrospinning

Mohammad Chowdhury · George Stylios

Received: 28 October 2010 / Accepted: 24 December 2010 / Published online: 6 January 2011

Abstract This paper describes the result of investigation on PVA/$FeCl_3$ nano composites fibres prepared by the electrospinning process. The effects of instrument parameters including solution concentration, electric voltage, tip–target distance, flow rate parameters on the morphology of electrospun PVA/$FeCl_3$ fibres were evaluated. The produced composite fibres were characterized by scanning electron microscopy (SEM) and transmission electron microscope (TEM). Fibre mats of (PVA)/$FeCl_3$ composite thin fibres, in the diameter of 500–1100 nm, were prepared by electrospinning. These microscopies show detailed morphologies of PVA/$FeCl_3$ nano composites incorporating magnetic power. These novel composite fibres could be used in biomedical, catalyst and magnetic purpose.

Introduction

Nanofibres have successfully been electrospun from different polymer systems such as organic polymers, high performance polymers, bio-polymers and polymer blends. The electrospinning process enables the formation of continuous nanofibres, composite fibres and align nanofibres [1, 2].

The electrospinning was first explored in the 1930s by Formhals as a simple and versatile method of making fibres from polymer solution with diameters typically ranging from 50 to 500 nm [3]. Current interests in nanostructured materials have stimulated renewed efforts in electrospinning. Nanofibre properties such as large area to volume ratio and high pore size make them suitable for adsorption of chemicals, military and civilian filtration application and aligned nanofibres in particular have potential applications in composite materials, in aerospace, automotive, reinforcements, electrochemical sensing, bone and blood vessel engineering and tissue engineering [4–6]. Melt spinning, solution spinning and gel state spinning are the common methods for polymer fibre production and these methods rely on mechanical forces to produce fibre by extruding a polymer melt or solution through a spinneret and subsequently drawing the resulting filaments as they solidify or coagulate; 5–500 micron diameter fibres can be produced by these methods [7, 8]. Electrospinning provides an interesting way to produce long polymer fibres with diameters in the range from 10 nm to a few microns. Nanofibre lengths depend on the time of electrospinning and can be a thousand of kilometres in a few minutes. Under room temperature, bending instabilities present in the polymer jet streams cause randomly oriented fibres with various diameters and structures during the electrospinning process [4, 9]. Poly(vinyl alcohol) (PVA) is a water-soluble polymer produced industrially by hydrolysis of poly(vinyl acetate). A number of grades of PVA are commercially available, which can be divided into two types: the fully hydrolyzed and the partially hydrolyzed PVA depending on the amount of acetate groups left in the backbone [10]. PVA is a semi-crystalline, hydrophilic polymer with good chemical and thermal stability, and is highly biocompatible, non-toxic and has high water permeability [11, 12]. The electrospinning of PVA solution and its potential applications in the preparation of ultrafine separation filters, biodegradable mats, etc. have been reported by many researchers [13, 14]. It has been reported that the common methods, such as melt spinning and dry or wet spinning, can only be used to prepare fibres/composites

M. Chowdhury (✉) · G. Stylios
Institute for Flexible Materials, School of Textiles and Design, Heriot-Watt University, Nethardale, Galshiels TD1 3HF, UK
e-mail: mmc6@hw.ac.uk

with diameters ranging from 5 to 500 μm [15]. Electrospun fibre mats of organic–inorganic hybrids such as PVA/silica and PVA/$H4SiMO_{12}O_{40}$ fibre mats were prepared and characterized by Shao et al. and Gong et al., respectively [16, 17]. Effect of molecular weight on electrospun fibrous PVA was discussed by Chuangchote and Supaphol [18]. Stabilization of fully hydrolyzed PVA fibres by treatment with methanol was investigated by Yao et al. [13] and PVA/Fe_3O_4 was discussed by Karim and Yeum [19]. In recent years, the focus of much scientific attention has been on the more biomedical applications of PVA hydro gels, including their uses in contact lenses, artificial organs and drug delivery systems [20]. However, other forms of electrospun fibres, such as uniaxially aligned arrays of as-spun fibres and single nanofibre, have been developed to expand their applications. To the best of our knowledge, five techniques for fabricating aligned fibres have been proposed: they are rotating drum collector technique [21], auxiliary electrode and electrical field technique [22, 23], spinning thin wheel with a sharp edge technique [24], frame collector technique [25] and multiple field technique [26]. This is an important step towards research and development (R &D) in controlled release of biomedical by using magnetic fields to manipulate the pore activity of the PVA with magnet transformed from $FeCl_3$.

This paper reports on the investigations done by the electrospun composites of PVA fibre filled with ferromagnetic nanoparticles. The importance of this nanocomposite system is due to the preparations of the filler nanoparticles are subjected to before electrospinning in order to obtain good dispersion in PVA fibre. The PVA/$FeCl_3$ composite fibres were characterized by microscopic technique. We have systematically evaluated the effects of instrument parameters, including solution concentration, electric voltage, tip–target distance, solution flow rate, on the morphology of electrospun PVA fibres, their alignment process.

Experimental methods

Materials and solution preparation

Poly(vinyl alcohol) (PVA), 99–100% hydrolyzed approx 86000 g/mol M_w was purchased from across organics, UK and $FeCl_3$ was purchased from Sigma-Aldrich, UK. PVA solutions (polymer concentrations ranging from 6 to 10% (g/mL)) were prepared by mixing the appropriate amount of polymer and water (milli-Q grade) at 100 °C under conditions of vigorous stirring until the polymer was completely dissolved. Solutions were stored at 80 °C overnight and were then cooled to room temperature. PVA Ferro gels (polymer concentration 6 to 10% g/mL and Ferro fluid concentrations ranging from 0 to 10% g/mL) were prepared by mixing the appropriate amount of $FeCl_3$ with aqueous PVA solutions. Homogenization was achieved at 90 °C under conditions of vigorous stirring. Samples were stored overnight at 80 °C and were then cooled to room temperature for 1 h, before being subjected to the electrospinning process.

Electrospinning setup

A Glassman MK35P2.0-22 (New Jersey, USA) high voltage DC power supply was used to generate potential differences of between 5 kV and 18 kV. One electrode of a high voltage was applied to a vertically (25-gauge) blunt-ended metal needle. The PVA polymer solution was fed from a syringe (5-mL capacity, Fisher Co, Leicestershire, UK) to a needle via Teflon® tubing and the flow rate was controlled using a digitally controlled, positive displacement syringe pump (Harvard Apparatus M22 PHD 2000, Eden bridge, Kent, UK), The electrospinning schematic diagram is shown in Fig. 1. Various polymer solution concentration ranging from 6 to 10 wt% were prepared by PVA with $FeCl_3$ mixtures. Fibres were obtained using an earthed collection system, which consisted of a copper collector plate measuring 15 cm × 15 cm. The operating flow rates were 0.20–0.30 mL/h at applied voltage between 12, 15, and 18 kV. Collection distances used during this experiment are 8, 11, and 14 cm.

Characterization

The samples produced for random nanofibres were collected on aluminium stubs. The morphology of the electrospun PVA/$FeCl_3$ fibres was observed with a scanning electron microscope (SEM), Model Hitachi S-530, UK and transmission electron microscope (TEM), Model JOEL JEM-2100F, UK. The diameter of the electrospun PVA/

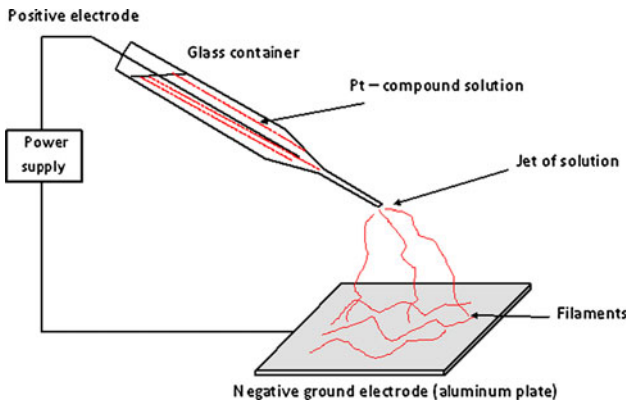

Fig. 1 A picture of the electrospinning set up

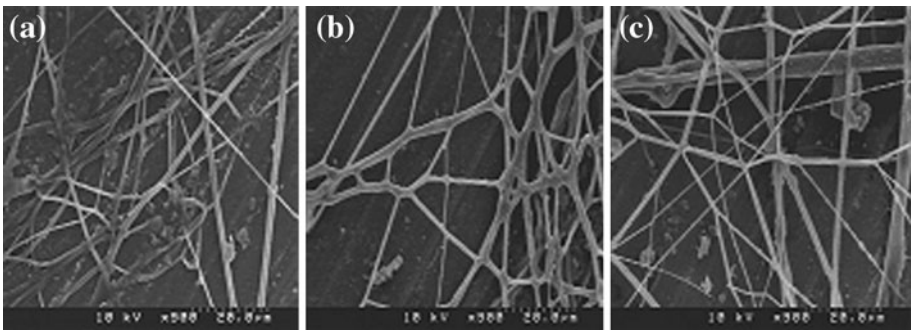

Fig. 2 SEM images of PVA/$FeCl_3$ where different polymer solution of **a** 6 wt%, **b** 8 wt% and **c** 10 wt% and constant applied voltage 15 kV, collecting distance 14 cm and flow rate 0.25 mL/h, respectively

$FeCl_3$ was investigated by an image analyzer (Image J, US).

Results and discussion

The effect of polymer concentration on fibre morphology

The diameter and morphology of electrospun nanofibres dependent on the solution concentration, the applied electric field strength, the tip-to-collector distance, etc. are the instrument parameters [1, 2, 27]. Among these parameters, the concentration or the corresponding viscosity of the electrospun solution was one of the most effective variables to control the fibre morphology and diameter of the PVA Ferro gels, which is in agreement with the work of others [28]. Solution concentration and viscosity are two closely correlated factors, increasing of solution concentration always results in increase of solution viscosity, and decrease of solution concentration always results in decrease of solution viscosity. A series of samples with different PVA/$FeCl_3$ concentrations were electrospun, resulting in various fibre morphologies and their diameter as shown in Figs. 2 and 3, at 6 wt% polymer solution the average fibre diameters was 735 nm and beads were observed. By increasing the polymer concentration the morphology was changed from beaded fibre to uniform fibre structure and the fibre diameter was also increased between 789 and 987 nm. In electrospinning, the coiled macromolecules of the solution are transformed by the elongational flow of the jet into oriented entangled networks that persist with fibre solidification. Below this concentration (less than 6 wt%) chain entanglements are insufficient to stabilize the jet driven by the surface tension caused the solution to form beads or beaded fibres. When the polymer solution increases at higher concentrations, viscoelastic forces which resist rapid changes in fibre shape result in uniform fibre formation. But if the solution concentration is too high, it would be impossible to electrospun because of their high viscosity. The changing of the

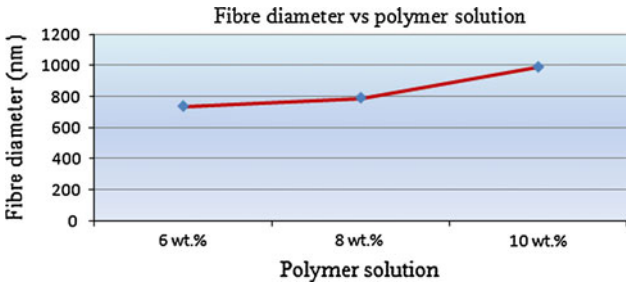

Fig. 3 Graphs describing the relationships between average fibre diameter and the polymer concentration

fibre morphology can probably be attributed to a competition between surface tension and viscosity. It has been found that viscosity and surface tension are the most important factors that effect the morphology of the resultant fibres and Reneker and Chun [1] also proved it in his experiment when he and his co-workers investigated the solution properties of poly(ethylene oxide) on the density of beads contained in the electrospun fibres. Vancso and coworkers have also indicated their research that smooth fibres can be formed when viscoelastic forces prevent the formation of beads [29]. Uniform fibres obtain higher concentration and lower concentration gives fibres with beads. If the concentration decreases bigger beads are obtained and some spot might be formed.

The effect of applied voltage on fibre morphology

The electrospinning process produces fibres only if the applied voltage is above a given limiting value required to overcome the surface tension of the solution. The electrical field is defined as the applied voltage divided by the distance between the tip and collector. Higher electric field values are obtained either through decreasing the distance between the tip and collector or by applying higher voltages. There exists controversy in the literature as to the effect of increasing the voltage on the final diameter of the electrospun nanofibre. A series of experiments were carried out by varying the applied voltage from 12 to 18 kV and tip to target distance at 14 cm. When the applied voltage

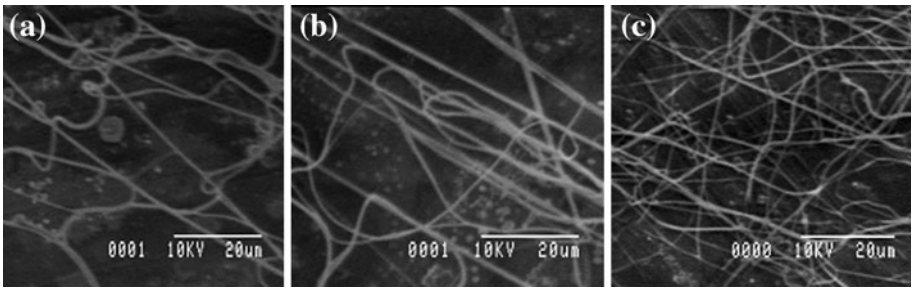

Fig. 4 SEM images of PVA/$FeCl_3$ at different voltages **a** 12 kV, **b** 15 kV and **c** 18 kV and constant polymer solution 8 wt%, collecting distance of 14 cm and flow rate of 0.25 ml/h, respectively

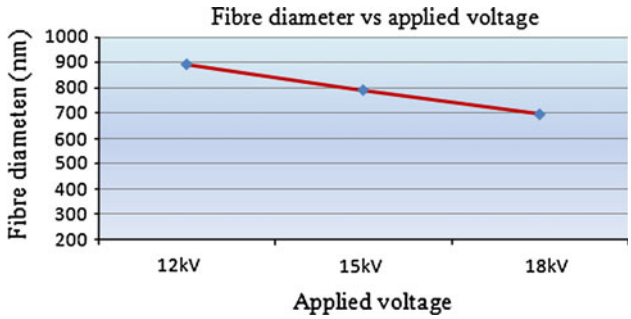

Fig. 5 Graph describing the relationship between average fibre diameter and applied electric voltage

increases the fibre diameter slightly increases. The applied voltage may effect some factors such as the mass of polymer fed from the tip of the pendant, the elongation level of jet and the morphology of the jet (single or multiple jets) [30–32]. A considerable amount of thin fibres with average diameters of 892 nm were found when the applied voltage was above 12 kV. At lower voltage narrow distribution of fibres were observed. At higher voltages of 15 kV to 18 kV more fibres were obtained. Increasing the applied voltage will increase the electrostatic repulsive force on the fluid jet which favours the thinner fibre formation. The average fibres calculate 791 nm to 696 nm. The solution will be removed from the capillary tip more quickly as jet is ejected from Taylor cone and thus making larger diameter fibres. As Figs. 4 and 5 show the SEM images of produced PVA/$FeCl_3$ blend fibres and relationships between the average fibre diameter and electric field with a constant concentration was 8 wt% and the collection distances of 14 cm. This figure shows that voltage played a part to produce uniform fibre diameter. It was observed that the diameter of the electrospun fibres was not dramatically changed with varied applied voltage. As the electric field strength increases, the electrostatically driven instability increases in magnitude that causes the jet to undergo higher amounts of whipping and plastic stretching that resulted in a decrease of the fibre diameter. It can be seen from Fig. 4 that exceedingly uniform fibre obtains lower voltage and the average diameter was 791 nm. Higher voltage gives more fibres but not uniformity like variation of the diameter of ultra fine fibre and its asymmetry distribution. The diameter of ultra fibres was reduced by increasing the voltage. And the graphs (Fig. 5) provided that, in general, increasing the applied voltage to a certain level would change the shape of the pendant drop from which the jet originated so that a stable shape could not be achieved. Finally, we can say that voltage effect has got a significant role to control the fibre morphology.

The effect of tip-to-collector distance on the fibre morphology

Tip to target distance is another process parameter for producing nanofibre by electrospun process. The most popular form of collected nanofibre is a nonwoven mat. The process enters an instability region and the fibres are distributed in a random formation. Tip to target distance actually makes no significant effect on the electrospun fibre morphology of fully hydrolyzed PVA and this phenomenon is not yet fully understood and is currently being researched. In order to investigate the effect of the distance between the needle and the collector on the properties of resulting ultra fine fibres, the following spinning condition were fixed. The voltage was fixed 18 kV and the concentration 8 wt% and distance 8, 11 and 14 cm. This result (Fig. 6) indicated that with varying size and thickness can be successfully produced. When the solution jets were elongated and solidified quickly they flowed out of the spinneret tip because of the high conductivity of fully hydrolyzed PVA and $FeCl_3$ used. At low separation distance between the capillary-end and the target, wet fibres were collected, primarily due to the presence of significant amount of residual solvent in the fibres. As the collection distance is increased, the time for the solvent to evaporate increased and as a result, dry solid fibres are collected at the target. With increasing the distance between the capillary-end and the target, the jet underwent a larger amount of electrically driven bending or whipping instability. Consequently, the amount of stretching or elongation of the jet increase results in the fibre diameter to decrease, which is in agreement with the results by Jalili et al. [33]. Figures 6 and 7 show the effect of the tip-to-collector distance.

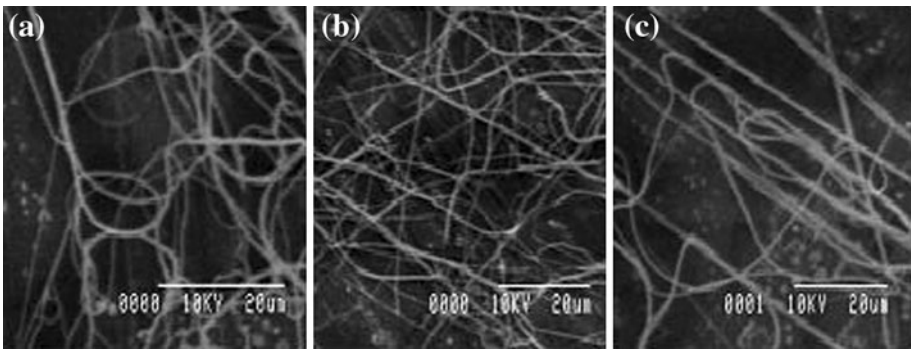

Fig. 6 SEM images PVA/$FeCl_3$ fibres at different collection gap distance **a** 8 cm, **b** 11 cm and **c** 14 cm with constant polymer solution 8 wt%, applied voltage (18 kV) and flow rate (0.25 mL/h), respectively

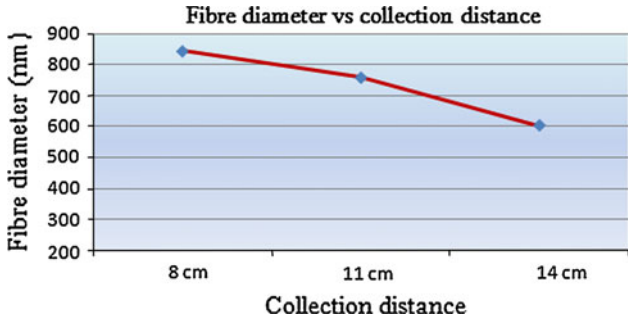

Fig. 7 Graph describing the relationships between the average fibre diameters and collecting distance

Considering Figs. 6 and 7, it is shown that at 8 cm collection distance the average fibre diameter of 845 nm was produced. Increasing the collection distance from 8 to 11 cm and 14 cm the fibre diameter decreases from 759 nm to 603 nm, respectively. It is stated that the fibres with smaller diameters are obtained by allowing the jet to cover more distance in the electric field. This also allows more time for the evaporation of the solvent from the fibres which also affects the decrease in fibre diameter. In this study, the most optimum tip-to-collector distance was found to be 14 cm resulting in uniform electrospun fibres.

The effect of flow rate on fibre morphology

The effect of flow rate on the morphological appearance of the fibres can be explained when considering the relationships among the three major forces (i.e., the Coulombic, the viscoelastic and the surface tension forces) influencing fibre diameter and bead formation. For a given applied potential, the electrostatic force, which carries a charged jet from the spinneret to the target, may increase slightly when compared with the increase in the feed rate as a result of an increase in the PVA/$FeCl_3$ solution flow rate. The excess amount of the material caused by an increase in the PVA/$FeCl_3$ flow rate results in the formation of a droplet at the tip of the spinneret. When the size of the droplet is too big to suspend at the tip of the spinneret, it either drops from the tip or it is carried along with a charged jet to the target. This ultimately provides in an increase of the bead area and of the diameter of the obtained fibres with increasing PVA/$FeCl_3$ flow rate, which can be observed qualitatively in Figs. 8 and 9.

Flow rate does not make any changes to solution properties such as viscosity, surface tension and conductivity. As flow rate increases, the feeding amount per unit time increases. From the volume conservation fibre diameter should increase. When the flow rate is 0.20 mL/h (Figs. 8, 9) the average fibre diameter observed is 564 nm. Increasing the flow rate from 0.20 mL/h to 0.25 mL and 0.30 mL/h increases the fibre diameter to 698 nm and 734 nm, respectively, as shown in Figs. 8b, c and 9. This is the similar result obtain by Fridrikh et al. [31]. At 0.20 mL/h flow rate bead formation is observed (Fig. 8), when the flow rate increases beads disappear. Other than bending instability, there can be a fluctuation of charge along the jet during electrospinning. If the charge density decreases at a specific spot instantaneously, surface tension surpasses the electrostatic repulsive force, because as flow rate increases, the electric current between metal needle and collector increases. Then the possibility to have instability decreases due to the increased electric current. With increasing the flow rate, more change is needed to initiate bead formation, hence bead formation is reduced as flow rate increase.

PVA/$FeCl_3$ align fibre

During the electrospinning process, the fibres are attracted to the grounded target. Because of the difference in the strength of the electric field and parallel target geometry, parts of fibres are deposited on two separate grounds simultaneously. Several techniques have been developed to align electrospun nanofibres and some breakthroughs have been obtained. The results are promising, but these methods need to be further improved for practical applications. The need of continuous fibre generation in the electrospinning necessitates continuous fibres between two targets with certain degree of orientation. The aligned fibre mats can be collected and processed into yarns for further application. A nanofibre alignment mechanism

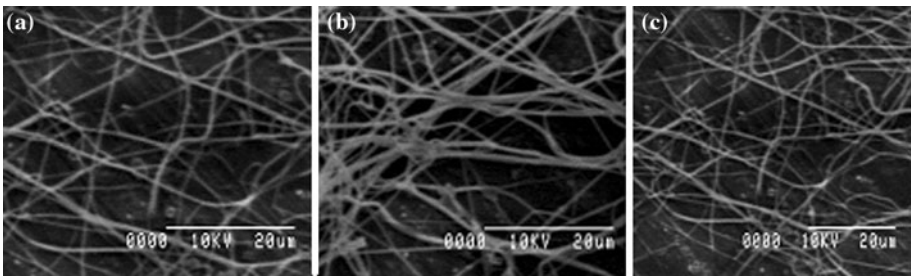

Fig. 8 SEM images of PVA/$FeCl_3$ fibres at different flow rates **a** 0.20 mL/h, **b** 0.25 mL/h and **c** 0.30 mL/h from constant polymer solution 8 wt%, under applied voltage (15 kV) and collection distance of 11 cm, respectively

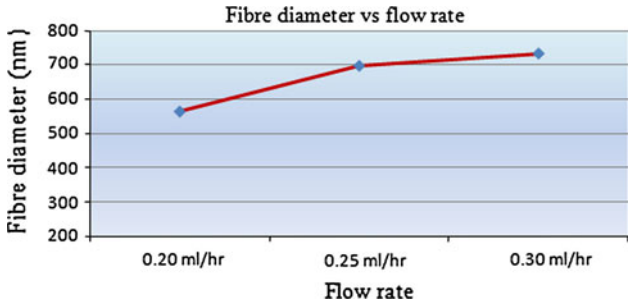

Fig. 9 Graph describing the relationships between the average fibre diameter and flow rate

involves collecting the electrically charged nanofibres between two faced electrically grounded collector discs. Two copper circular discs (28 mm OD, 2 mm thick) are used as a collection discs. They were positioned by grounded alligator clips, with the top of the discs being 8 cm away from the spinneret. In this process, when placing the two grounded discs under the collection distance the vertical electric field lines are split into two parts. The geometrical shape of the electric field and then aligns the electrospun nanofibres between the two discs. Producing PVA/$FeCl_3$ align nanofibres with a concentration of 6, 8 and 10 wt%, applied voltage of 15 kV, volume feed rate of 0.20 mL/h and the collection distance of 8 cm reduced the diameter of the fibres from micrometer to the submicron range and the diameter was adjusted by controlling the stretching ratio.

There is a demand for methods of alignment of nanofibres in one or few directions. Electrospun fibre is directly deposited onto a grounded collector as a random mesh and in a second two copper discs was covered by a long fibres bundles and it curved parallel path between the two discs as shown in Fig. 10a. Figure 10b shows that aligned nanofibres are at the right angles to the axis of the collection discs and have a uniform diameter distribution. Electrostatic interactions between the positive electrode on the spinneret and the ground disk made the fibres aligned and stretched. As a result the polymer fibres travel toward the disk collector, one end of the fibre is attached to one of the discs and the other end of the fibre is gathered towards the other disk. The bending shape of the flying nanofibres is transformed into a linear shape between the grounded circular discs. When the charged fibres moved into the gap between the discs, the fibres will induce opposite charges on the surface of the discs. This opposite charges will attract the fibres to the grounded discs, leading to the alignment of the fibres in the gap between the circular discs. The nanofibres suspended across the gap remain highly charged after deposition, thus the electrostatic repulsion between the deposited and upcoming fibres can further improve the alignment mechanism. The morphological structure of aligned electrospun PVA/$FeCl_3$ fibres obtained from the 6–10 wt% polymer solution is shown in Fig. 11. The SEM images in Fig. 11 show that well-aligned nanofibres have been formed. The average aligned fibre diameters are 560, 625 and 750 nm. It was also noticed that the average diameter of aligned fibres was smaller than that of the random fibres obtained from the same processing conditions. The aligned fibres collected have lower average fibre diameters because their reduction and expansion values are lower than in the case of random collection, leading to a decrease in the fibre diameter.

This experiment shows that the number of nanofibres distributed in the bundle depends on parameters such as the collection time and the gap width. However, the applied voltage, spinning distance and flow rate are the main parameters effect on the mass of the deposited fibres and the number of branches generated from the electrospinning jet. When the applied voltage increases the nanofibre branching also increases and it makes the PVA/$FeCl_3$ nanofibre alignment difficult. It also increases the alignment across the gap because the voltage will increase the drawing forces. The images in Fig. 11 show that as the deposition time increased and the width of the gap decreased, the number of PVA/$FeCl_3$ fibres increase and this makes the bundle closer. This result is in agreement with the result of Morshed et al. [34].

TEM observation of the produced PVA/$FeCl_3$ composite fibres

TEM images of the PVA/$FeCl_3$ electrospun fibres are shown in (Fig. 12). After electrospinning, Ferro gel particles were distributed in a matrix formed by PVA. This

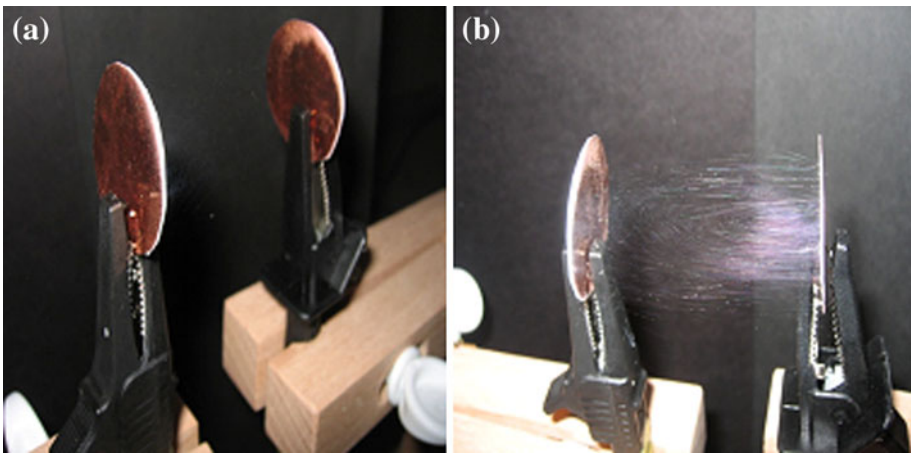

Fig. 10 Shows the experimental setup for produce align nanofibres (**a**, **b**)

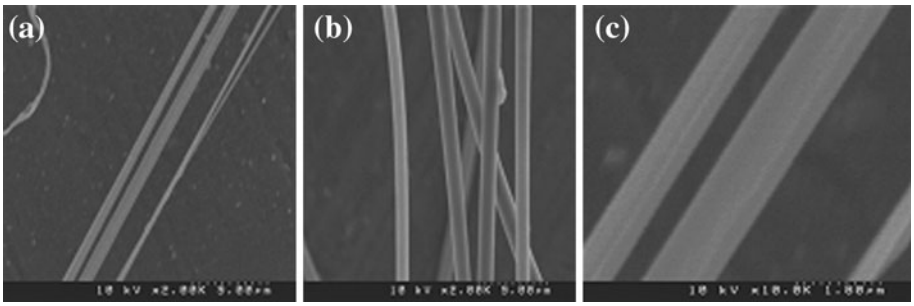

Fig. 11 SEM images of PVA/$FeCl_3$ nanofibres where the collection time is 60 s and disk gap of 4 cm and solution were **a** 6 wt%, **b** 8 wt% and **c** 10 wt%

confirms the presence and distribution of Ferro particles in the electrospun nanocomposites.

As shown in the figures, localized particle agglomerations were also observed. The agglomerated particles were more often found from the fibres fabricated using lower concentration of Ferro gel solution. Overall fibres were found to possess Ferro particles in and on the fibres. Figure 12a–d shows TEM images of PVA/$FeCl_3$ nanofibre containing Ferro particles. Ferro particles appeared as little dark spots inside of the nanofibres 6 wt% concentration and produced agglomerated fibre, when concentration increased from 6 to 8 wt% that time the fibre diameter also increased and beads free uniform fibre was produced. From Fig. 12a, b we can see that Ferro gel aligned distributed. Figure 12d showed the Ferro particle clearly where uniform fibre was produced.

Magnetic nanofibres

From the above condition we got a blended fibre where the fibre contains magnetic power. The electrospun blend nanofibres have unique magnetic properties, with much enhanced coercivities relative to bulk materials. The outstanding features of this approach to get one-dimensional magnetic nanostructure are its simplicity, effectiveness, and ease of assembly. Therefore, electrospun magnetic nanofibres can potentially be used in fabrication of high-density magnetic recording, magnetic sensors, flexible magnets, and spintronic devices, which can be seen from Fig. 13.

Conclusion

Electrospinning was used to fabricate nanofibres of PVA/$FeCl_3$ blends. The effect of processing parameters such as, the solution concentration, the voltage, the tip–target distance and flow rate on fibre and its morphology has been examined and magnetic fibre produced. The electrospinning of PVA/$FeCl_3$ solution was processed and fibres with diameter ranging from 500 to 1100 nm were obtained depending on the electrospinning conditions. The effects of the concentration, spinning voltage and collection distance between the tip to target on the morphological appearance and average diameter of the PVA/$FeCl_3$ fibre and aligned fibre was also investigated. It was concluded that the solution concentration significantly affected the morphology and diameter of the PVA/$FeCl_3$ nanofibres. Lower concentration tended to facilitate the formation of fibres with beads. As the solution concentration, the morphology was changed from beaded fibres to smooth and uniform nanofibre and with increasing fibre diameter. The spinning voltage had also an important influence on fibre diameter,

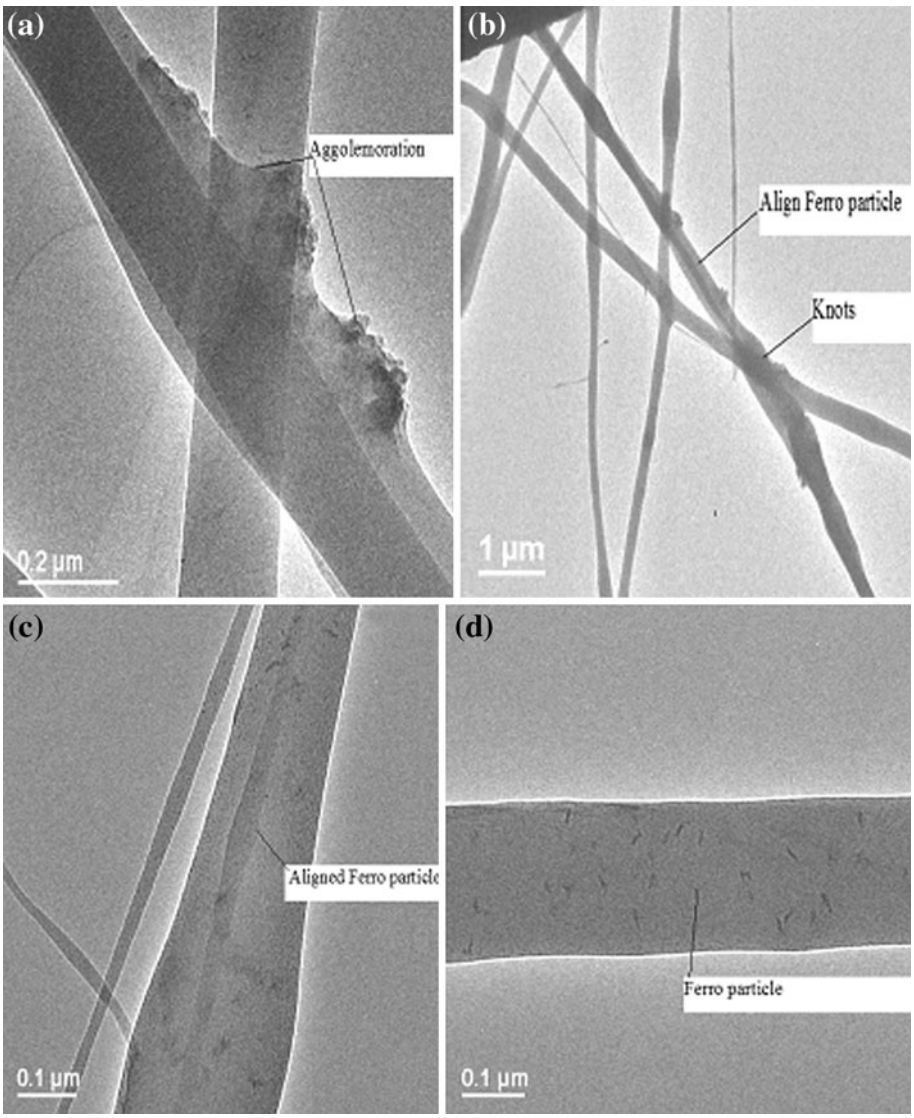

Fig. 12 Transmission electron microscopy images of PVA/$FeCl_3$ composite nanofibres **a** 6 wt%, **b** 8 wt%, **c** 8 wt% and **d** 10 wt%

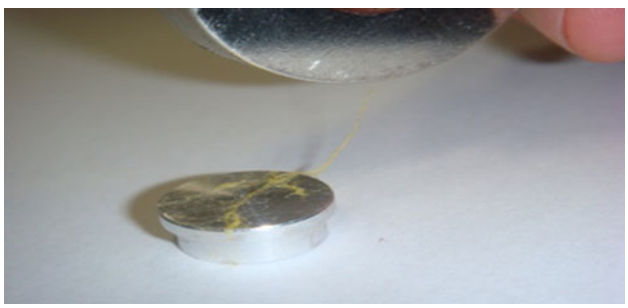

Fig. 13 PVA/$FeCl_3$ blend nanofibres with magnet, it shows the magnetic power of the blended fibre

while the collection distance had a lesser effect on the fibre diameter. Finer fibres with highly uniformity with the application of lower voltage. Aligned fibre also produced and Ferro particles identified. The produced magnetic nanofibres can potentially be used in fabrication of high-density magnetic recording, magnetic sensors, flexible magnets and spintronic devices.

References

1. Reneker DH, Chun I (1996) Nanotechnology 7:216
2. Huang ZM, Zhang YZ, Kotaki M, Ramakrishna S (2003) Compos Sci Technol 63:223
3. Formhals A (1934) US Patent No. 1975504
4. Chase GG, Ramsier RD, Alessandro M, Katta P (2003) Nano Lett 4(11):2215
5. Doshi J, Reneker DH (1995) J Electrost 35:151
6. Bershoef MM, Vancso GJ (1999) Adv Mater 11:1362
7. Edwards WM (1965) US Patent No. 3415782
8. Irwin RS (1968) US Patent No. 3415782
9. Yarin AL, Zussman E, Theorn SA (2004) Eur Polym J 45:2017
10. Mark HF, Gayload NG (1980) Encyclopedia of polymer science and technology, vol 14. Wiley, New York

11. Krumova M, Lopez D, Benavente R, Mijangos C, Perena JM (2000) Polymer 41:9265
12. Shivkumar S, Yim K, Koski A (2004) Mater Lett 58:493
13. Yao L, Haas TW, Elie AG, Bowlin GL, Simpson DG, Wnek DG (2003) Chem Mater 15:1860
14. Koski A, Yim K, Shivkumar S (2004) Mater Lett 58:4939
15. Deitzel JM, Kleinmeyer J, Harris D, Beck Tan NC (2001) Polymer 42:261
16. Shao CL, Kim HY, Gong J, Ding B, Lee DR, Park SJ et al (2003) Mater Lett 57:1579
17. Gong J, Li XD, Ding B, Lee DR, Kim HY (2003) J Appl Polym Sci 89:1573
18. Chuangchote S, Supaphol P (2006) J Nanosci Nanotechnol 6:125
19. Karim M, Yeum JH (2010) Soft Mater 8(3):197
20. Sona WK, Youkb JH, Lee TS (2005) Matter Lett 59:1571
21. Jayaraman K, Kataki M, Zhang Y, Mo X, Ramakrishna S (2004) J Nanosci Nanotechnol 4:52
22. Bornat A (1987) US Patent 4689186
23. Berry JP (1990) US Patent 4965110
24. Theron A, Zussman E, Yarin AL (2001) Nanotechnology 12:384
25. Deitzel JM, Kleinmeyer JD, Hirvonen JK, Tan NC (2001) B-Polymer 42:8163
26. Kameoka J, Czaplewski D, Liu H, Craighead HG (2004) J Mater Chem 14:1503
27. Bognitzki M, Czado W, Frees T, Schsper A, Hellwig M, Steinhart M (2001) Adv Mater 13(1):70
28. Zong XH, Kim KS, Fang DF, Ran SF, Hsiao BS, Chu BJ (2002) Polymer 43(16):4403
29. SY GU, Ren J, Vancso GJ (2005) Eur Polym J 41:2559
30. Tan SH, Inai R, Kotaki M, Ramakrishna S (2005) Polymer 46:6128
31. Fridrikh SV, Yu JH, Brenner MP, Rutledge GC (2003) Phys Rev Lett 90:144502
32. Wan T, Chowdhury M, Stylios G (2010) Mater Sci Forum 650:361
33. Jalili R, Hosseini SA, Morshed M (2005) Iran Polym J 14:1074
34. Jalili R, Morshed M, Ravandi SAH (2006) J Appl Polym Sci 101:4350